Compact Optical Modulator based on Carrier Induced Gain of an InP/InGaAsP Micro-disk Cavity Integrated on SOI

Liu Liu*[a], Joris Van Campenhout[b], Günther Roelkens[a], Richard Soref[c], Dries Van Thourhout[a], Pedro Rojo-Romeo[d], Philippe Regreny[d], Christian Seassal[d], Jean-Marc Fédéli[e], Roel Baets[a]

[a]Photonics Research Group, Department of Information Technology (INTEC), Ghent University—IMEC, St-Pietersnieuwstraat 41, 9000 Ghent, Belgium;

[b]Currently with IBM T. J. Watson Research Center, 1101 Kitchawan Rd., Yorktown Heights, NY 10598, USA;

[c]Air Force Research Laboratory, Sensors Directorate, Hanscom AFB, MA 01731, USA;

[d]Université de Lyon; Institut des Nanotechnologies de Lyon INL-UMR5270, CNRS, Ecole Centrale de Lyon, Ecully, F-69134, France;

[e]CEA/Léti—Minatec, 17 rue des Martyrs, 308054 Grenoble, France

ABSTRACT

A compact electro-optic modulator on silicon-on-insulator is presented. The structure consists of a III-V microdisk cavity heterogeneously integrated on a silicon-on-insulator wire waveguide. By modulating the loss of the active layer included in the cavity through carrier injection, the power of the transmitted light at the resonant wavelength is modulated. ~10 dB extinction ratio and 2.73 Gbps dynamic operation are demonstrated without using any special driving techniques. The results are consistent with the theoretical simulations.

Keywords: silicon-on-insulator, heterogeneous integration, electro-optic modulator, carrier injection

1. INTRODUCTION

Silicon-on-insulator (SOI), an emerging platform for optical interconnections, has attracted considerable research interest in recent years, largely motivated by its CMOS compatible fabrication process, and the possibility to integrate with electronic circuits [1]. One example of this type of integrated devices is an electro-optic modulator on SOI. The refractive index of silicon can be modified through carrier injection or depletion [2-8]. This effect, so-called the free carrier dispersion (FCD) [9], is so far the best all-silicon solution to achieve a fast and efficient optical modulator on SOI, due to the fact that silicon exhibits very weak or even zero coefficients of other common electro-optic effects, e.g., the Pockels effect, the Kerr effect, and the Franz-Keldysh effect. Devices based on carrier depletion can offer a fast operation speed. 40 Gbps bit rate has been demonstrated, recently [4]. However, due to the small light confinement in the depleted region, the interaction length of the device has to be large (e.g., in the order of millimeter [2-4]), or a high drive voltage is required, to ensure enough modulation depth. On the other hand, carrier injection approach can improve the modulation efficiency, but the speed is limited by the slow carrier injection/recombination processes in silicon [5-8]. Based on carrier injection, <1 Gbps nonreturn-to-zero (NRZ) modulation has been reported originally [5, 6], and ~10 Gbps has been achieved by using the pre-emphasis driving technique [7, 8].

III-V compound semiconductors can provide a variety of electro-optic effects for light modulation, and they are often much faster and stronger than those in silicon. Heterogeneous integration of the III-V active material with the silicon passive waveguide would be a promising approach to improve the performance of such a modulator on SOI. Recently, a hybrid silicon evanescent modulator with a length of several hundred microns has been proposed employing the electro-absorption effect in a III-V multiple-quantum-well region bonded on top of an SOI waveguide [10]. In this letter, we introduce a carrier-injection-based microdisk modulator on the heterogeneous III-V/SOI platform. By using a resonant structure, the dimension of the proposed device is shrunk below 10 um. Different from the FCD employed in the all-

* liu.liu@intec.ugent.be; phone +32-9-2648930; fax +32-9-2643593

Optoelectronic Materials and Devices III, edited by Yi Luo, Jens Buus, Fumio Koyama, Yu-Hwa Lo
Proc. of SPIE Vol. 7135, 71351I · © 2008 SPIE · CCC code: 0277-786X/08/$18 · doi: 10.1117/12.803085

silicon approaches, the working principle here is based on the fact that the loss/gain of the active material in the microdisk cavity (MDC) varies with current injection. >10 dB extinction ratio and 2.73 Gbps operation speed are achieved in the proposed device without using any special driving techniques.

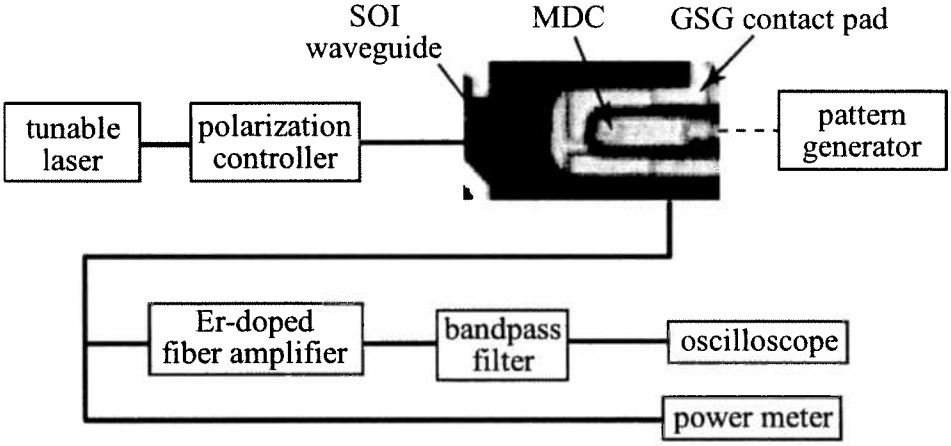

Fig. 1. Experimental setup for electro-optic modulation and a microscope picture of the employed microdisk cavity.

2. FABRICATION AND EXPERIMETNTAL SETUP

Figure 1 shows a sketch of the experimental setup. The cavity was formed by a III-V microdisk with a diameter of 7.5 um and a thickness of 1 um. This III-V layer was bonded on top of an SOI wire waveguide (dimension: 500×220 nm^2) prior to the definition of the disk. A p-i-n diode with three strained InAsP quantum wells (absorption edge at ~1620 nm) was embedded in this III-V layer along the vertical direction for carrier injection. We refer to Ref. [11] for detailed epi-layer structure and the corresponding parameters. The microdisk is driven by a voltage signal directly from a pattern generator through a high-speed ground-signal-ground (GSG) probe. Transverse-electric (TE) polarized light from a tunable laser was coupled into the SOI waveguide. The input light then interacted with the whispering-gallery mode (WGM) circulating around the perimeter of the MDC through vertical evanescent coupling. The WGM experiences either a loss or a gain depending on the bias current. The transmitted light in the SOI waveguide was collected. For dynamic measurements, it was first amplified by an Erbium-doped fiber amplifier (EDFA), and a bandpass filter was employed to suppress the spontaneous emission noise.

3. STATIC MEASUREMENT RESULTS

The working principle of the proposed modulator is as follows. When no current is injected, the intrinsic loss of the III-V microdisk is high for the light propagating in the SOI waveguide, as compared to the coupling strength between them. Thus, The MDC is actually working in an under-coupled regime [12]. There would be no obvious resonance absorption for the transmitted light. When a current is injected, the loss of the micro-disk is partially compensated by the gain from the active layer due to the carrier injection. In this case, the MDC could be critically coupled. Therefore, at the resonance wavelength, all the light would be dropped in the MDC.

Figure 2 shows the static transmission measurement results with different bias voltages/currents. The MDC was always driven below its lasing threshold, which is 800 uA. As we can see, at zero bias, no resonance dip is observed. As the current increases, the resonance becomes more and more obvious, and the line width decreases as well due to the reduced losses. The best extinction ratio of about 19dB is obtained at 1.18V/540μA. Further increasing the current makes the extinction ratio drop, meaning that the MDC probably works in an over-coupled regime. The bias current used here is still high (hundreds of μA), as compared to the all-silicon ring modulator (tens of μA) [5, 6]. This is partially due to the disk structure employed. Since the optical field is confined at the edge of the micro-disk, the current going through the center part is wasted. Actually, the current density in these two cases is at the same level. Therefore, a significant decrease of the power consumption is expected by, e.g., creating a hole in the center of the disk to block the unnecessary current, or employing an ultrasmall disk as demonstrated in [13]. Reducing the number of quantum wells and, in the meantime, the disk thickness (to ensure the same light confinement in the quantum wells) can also decrease the current.

Besides through carrier injection as proposed here, the loss of a III-V active layer can also be modified via a fast field effect, e.g., the electro-absorption effect under a reverse bias [9]. This can largely reduce the power consumption. The insertion loss of the device is expected to be ~3 dB due to the coupling to the higher order mode supported by the 1 um thick III-V layer [14].

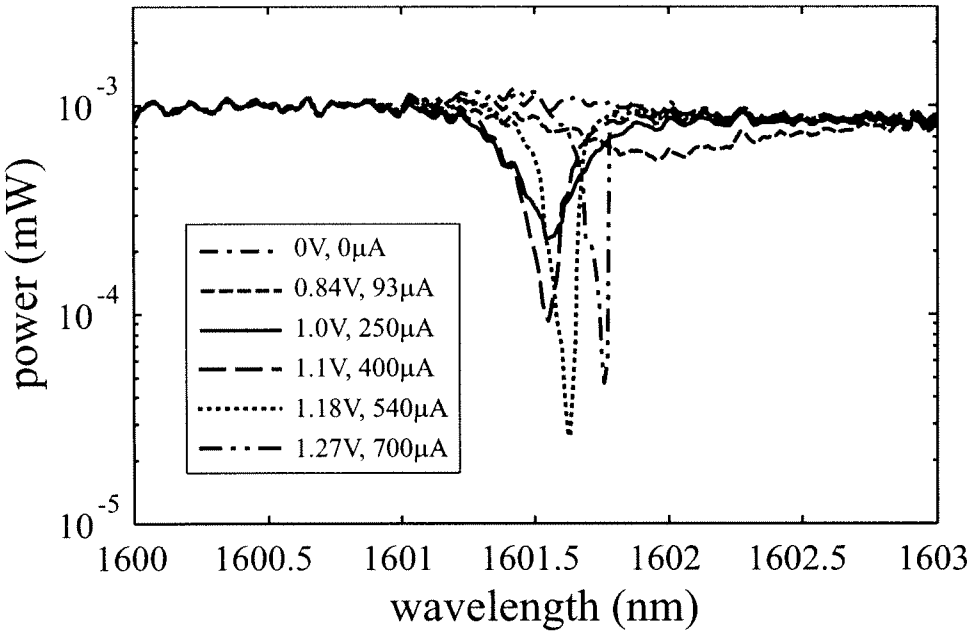

Fig. 2. Static transmission spectra through the MDC with different bias voltages and currents. The lasing threshold current of the MDC is 800 uA.

Table. 1. Material parameters and corresponding values.

Parameter	Value	Parameter	Value
Injection efficiency (η)	0.81	Elementary charge (q)	1.6×10^{-19} C
Microdisk radius (R)	3.75 um	Active layer thickness (t_a)	15 nm
Shockley-Read-Hall (SRH) recombination coefficient (A)	1×10^{8} s^{-1}	Spontaneous recombination coefficient (B)	1.6×10^{-10} cm^3/s
Auger recombination coefficient (C)	7.5×10^{-28} cm^6/s	Active layer confinement fact (Γ)	3.89%
Gain coefficient (G_0)	1500 cm^{-1}	Transparent carrier density (N_{tr})	1.5×10^{18} cm^{-3}

In order to analyze the above static results, we employ the following rate equation to model the dynamics in MDC [13]:

$$\frac{dN}{dt}=\frac{\eta I}{q\left(\pi R^2 t_a\right)}-\left(AN+BN^2+CN^3\right), \tag{1}$$

where, N is the carrier density in the MDC, and I is the bias current. Here, we ignored the stimulated recombination of the carrier due to the injected photons in the cavity. Please refer to Sec. 0 for further discussions about this effect. The relation between the mode gain G of the WGM and the carrier density N in the MDC can be expressed as follow [13]:

$$G = \Gamma G_0 \ln\left(\frac{N}{N_{tr}}\right). \tag{2}$$

The meanings of other parameters in Eqs. (1)-(2), as well as the corresponding values, are all denoted in Tab. 1.

A time-domain coupled-mode theory is used to analyze the interaction of the cavity resonance with the SOI waveguide mode [15]. The relation between the transmission T and the frequency ω of the input laser is expressed as:

$$\begin{aligned} T &= \left| 1 - \frac{\frac{1}{\tau_c}}{j(\omega-\omega_0) + \frac{1}{2\tau_i} + \frac{1}{2\tau_c}} \right|^2 \\ &= \left| 1 - \frac{v_g \alpha_c}{j(\omega-\omega_0) + \frac{v_g(\alpha_o - G)}{2} + \frac{v_g \alpha_c}{2}} \right|^2, \end{aligned} \tag{3}$$

where, ω_0 is the resonant frequency, $v_g=c_0/n_g$ is the group velocity of the WGM (c_0 is the light speed in vacuum and n_g =3.4 is the group index), α_c is distributed coupling loss between the MDC and the SOI waveguide, α_o is the loss of the WGM, which includes the scattering loss, the radiation loss, the free carrier absorption loss due to doping, etc., but excludes the gain of the active layer (G). The best fitting for the results in Fig. 2 by using Eq. (3) gives α_c=5.5 cm^{-1} and α_o = 11.3 cm^{-1}, which is close the values reported in Ref. [11]. The relation between the mode gain G and the bias current can also be obtained by the above fitting. The data is plotted in Fig. 3 together with the theoretical calculation from Eqs. (1) and (2). Two results show good agreement.

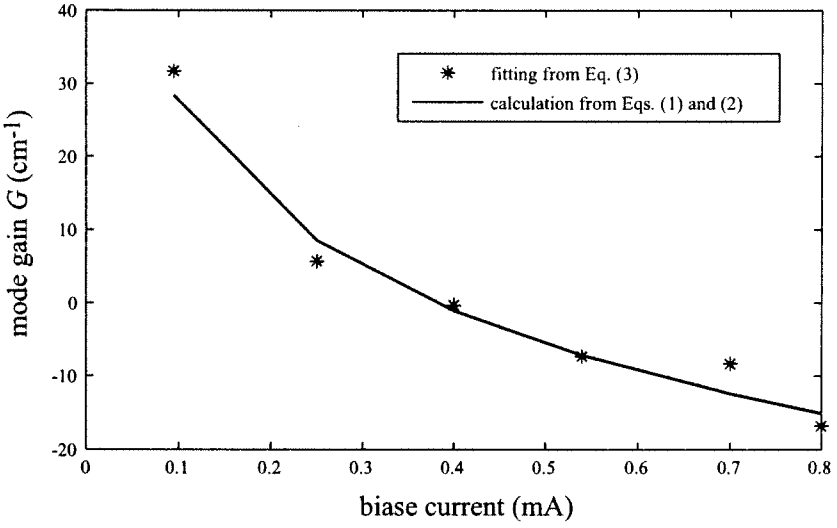

Fig. 3. Relation between the mode gain G and the bias current. Stars show the fitting data of the static results in Fig. 2 by using Eq. (3). Solid line shows the theoretical calculation from Eqs. (1) and (2).

It is worthwhile to note that the positions of the transmission dips also vary under different bias conditions in Fig. 2. This dip first blue-shifts as the current increases due to the increase of the carrier density in the active layer, similar to the FCD effect employed in the all-silicon modulators [5-8]. As the bias increases further, the thermo-optic effect starts to take over, and a red-shift is therefore observed. The thermal resistance of the proposed was measured to be 9 K/mW [16]. Assuming the thermo-optic coefficient of the III-V material to be 0.1 nm/K, we can deduce the resonant wavelength shift due to the pure FCD effect $\Delta\lambda_{FCD}$ from that due to the thermo-optic effect $\Delta\lambda_{th}$ (the total wavelength shift $\Delta\lambda = \Delta\lambda_{FCD} + \Delta\lambda_{th}$). The results are plotted in Fig. 4. From Eqs. (1) and (2), we can also calculate the FCD-induced resonant wavelength shift theoretically with the following relations [17]:

$$\Delta\lambda_{FCD} = -\Delta G \cdot \frac{\pi \cdot c_0^2}{\omega_0^2 \cdot n_g} \cdot \alpha \,, \tag{4}$$

where, ΔG is the mode gain variation, and α is the line width enhancement fact [16]. A good match between the result from Eq. (4) and the deduced resonant wavelength shift excluding the thermo-optic effect can be obtained by taking α=4, which is a typical value of the active material used in the proposed devices [13, 17].

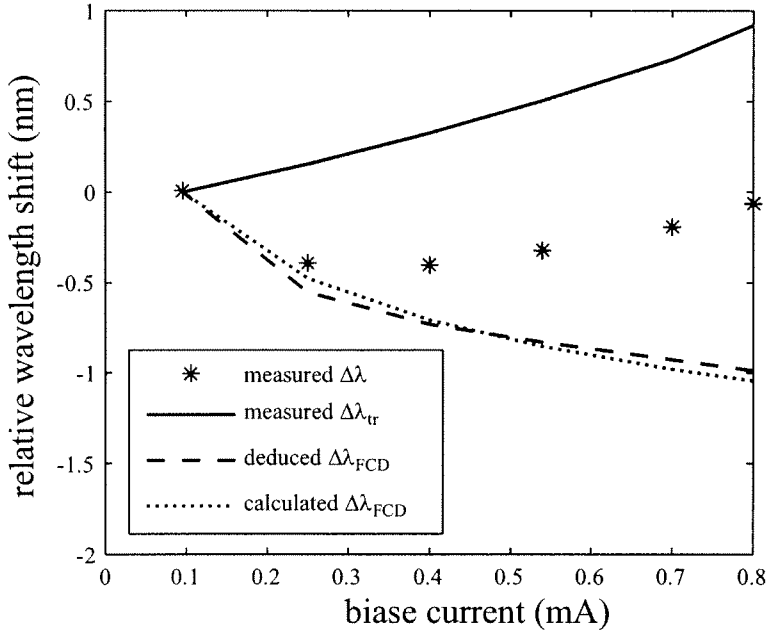

Fig. 4. Relative wavelength shift as a function of the bias current. Stars show the measurement total wavelength shift $\Delta\lambda$ from Fig. 2. Solid line denotes the measured wavelength shift $\Delta\lambda_{th}$ due to thermo-optic effect. Dashed line denotes the deduced wavelength shift $\Delta\lambda_{FCD}$ due to the FCD effect from the above two values. Dotted line denotes the calculated $\Delta\lambda_{FCD}$ from Eqs. (1) , (2) and (4).

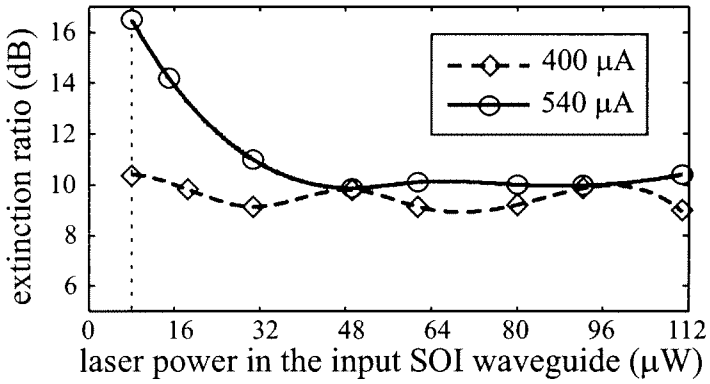

Fig. 5. Measured extinction ratio as a function of the laser power in the input SOI waveguide. Parameters are the bias currents. The dotted line denotes the power level used in Fig. 2.

4. EFFECT OF THE INPUT LASER POWER

In the above analysis, we ignored the impact of the input laser power. Indeed, the stimulated excitation or recombination of the carriers caused by the resonant photons in the MDC would affect the value of G, as well as the transmitted power. To study this effect, we recorded the extinction ratios at different input power levels, and the results are shown in Fig. 5. For 540 uA bias the extinction ratio drops obviously as the input power increases, and it is saturated around 10 dB. While, for 400 uA bias the extinction ratio is rather stable within 10 dB±1 dB at different power levels. This can be explained if the active layer is at transparency (i.e., G=0) at 400 uA bias. In this case, no stimulated excitation or recombination occurs. Thus, G and the extinction ratio are not affected by the input power. While, at a higher bias the active layer exhibits a gain (i.e., G>0). The stimulated recombination of the carriers gradually saturates this gain due to the increased photon density in the MDC, and G increases back to 0 at a high laser power. As a result, the extinction ratio drops to the value at transparency, i.e., ~10 dB. Similar behavior was also observed at a lower bias, where the extinction ratio increases as the input power increases due to the absorption bleaching of the active layer. For a practical modulator, the modulation depth should not depend on the input laser power. Therefore, we can conclude that the best operation point for the proposed device should be at 400 uA injection current.

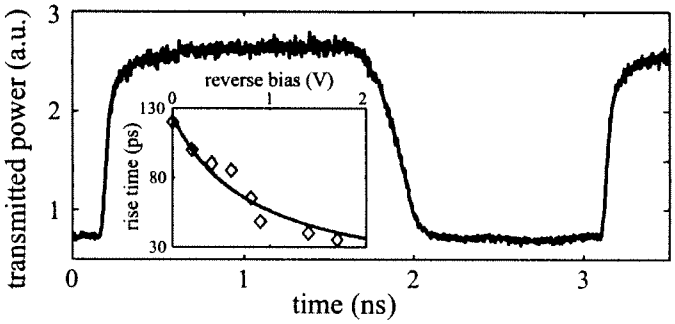

Fig. 6. Optical response of the modulator under a square wave signal with a voltage level of 0 V–1.1 V and a frequency of 340 MHz. Inset shows the rise time as a function of the reverse bias voltage.

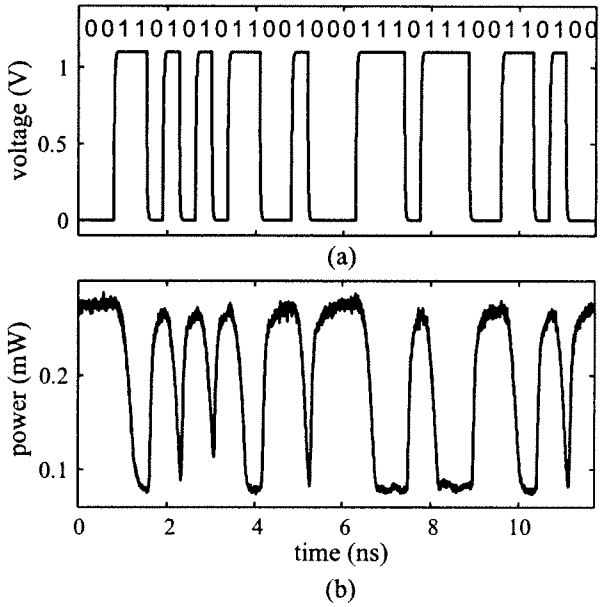

Fig.7. Waveform of a 32-bit NRZ signal at 2.73 Gbps applied on the proposed modulator (a), and the corresponding optical signal (b).

5. DYNAMIC MEASUREMENT RESULTS

The dynamic result of the optical modulation is shown in Fig. 6, where the MDC was driven with a radio frequency (RF) electric signal directly from the pattern generator. The electric driving signal was a square wave from 0 V to 1.1 V at frequency of 340 MHz. The extinction ratio is about 6 dB, slightly less than the static results (10 dB for 1.1 V bias), due to the significant spontaneous emission from the EDFA. The measured rise and fall time of the modulated light are about 120 ps and 350 ps, respectively, which are faster than those of the all-silicon based modulators, where these transition time is usually in the order of nano-second [5, 6]. Employing a reverse bias (instead of 0 V) could increase the carrier extraction speed, and hence make the rising edge shaper. As show in the inset of Fig. 6, a 35 ps rise time can be obtained with a -1.8 V bias. However, the speed of the proposed device here is mainly limited by the much slower fall time, i.e., the slow carrier injection dynamics. Thus, the reverse bias technique was not adopted in this paper. Note that the pre-emphasis driving technique could also be introduced here to increase the carrier injection speed, as it has been demonstrated for the all-silicon ring modulator [7, 8]. In Fig. 7, we further show the waveform of the electric driving signal using a 32-bit NRZ pattern, as well as the corresponding optical signal, at a bit rate of 2.73 Gbps. As we can see, the information was reversely transferred onto the laser beam.

6. CONCLUSION

We have introduced an electro-optic modulator with a III-V MDC heterogeneously integrated on an SOI wire waveguide. By modulating the bias current, the active layer in the MDC works between a high loss and transparency. Therefore, the drop efficiency of the cavity, as well as the power of the transmitted light, is also modulated. ~10 dB extinction ratio and 2.73 Gbps dynamic operation have been demonstrated without using any special driving techniques. A rate equation based model has been employed to analyze the static results. Good agreement has been obtained.

REFERENCES

[1] W. Bogaerts, R. Baets, P. Dumon, V. Wiaux, S. Beckx, D. Taillaert, B. Luysseart, J. Van Campenhout, P. Bienstman, and D. Van Thourhout, "Nanophotonic waveguides in silicon-on-insulator fabricated with CMOS technology," J. Lightwave Technol. 23(1), 401-412 (2005).

[2] A. Liu, R. Jones, L. Liao, D. Samara-Rubio, D. Rubin, O. Cohen, R. Nicolaescu, M. Paniccia, "A high-speed silicon optical modulator based on a metal-oxide-semiconductor capacitor," Nature 427 (12), 615-618 (2004).

[3] A. Liu, L. Liao, D. Rubin, H. Nguyen, B. Ciftcioglu, Y. Chetrit, N. Izhaky, and M. Paniccia, "High-speed optical modulation based on carrier depletion in a silicon waveguide," Opt. Express 15 (2), 660-668 (2007).

[4] L. Liao, A. Liu, D. Rubin, J. Basak, Y. Chetrit, H. Nguyen, R. Cohen, N. Izhaky, and M. Paniccia, "40 Gbit/s silicon optical modulator for high speed applications," Electron. Lett. 43(22), 1196-1197 (2007).

[5] Q. Xu, B. Schmidt, S. Pradhan, and M. Lipson, "Micrometre-scale silicon electro-optic modulator," Nature 435(19), 325-327 (2005).

[6] L. Zhou and A. W. Poon, "Silicon electro-optic modulators using p-i-n diodes embedded 10-micron-diameter microdisk resonators," Opt. Express 14(15), 6851-6857 (2006).

[7] Q. Xu, B. Schmidt, J. Shakya, and M. Lipson, "12.5Gbit/s carrier-injection-based silicon microring silicon modulators," Opt. Express 15(2), 430-436 (2007).

[8] W. M. J. Green, M. J. Rooks, L. Sekaric, and Y. A. Vlasov, "Ultra-compact, low RF power, 10 Gb/s silicon Mach-Zehnder modulator," Opt. Express 15(25), 17106-17113 (2007).

[9] R. A. Soref and B. R. Bennett, "Electrooptical Effects in Silicon," IEEE J. Quantum Electron. 23(1), 123-129 (1987).

[10] Y. Kuo, H. Chen, and J. E. Bowers, "High speed hybrid silicon evanescent electroabsorption modulator," Opt. Express 16(13), 9936-9941 (2008).

[11] J. Van Campenhout, P. Rojo-Romeo, P. Regreny, C. Seassal, D. Van Thourhout, S. Verstuyft, L. Di Cioccio, J.-M. Fedeli, C. Lagahe, and R. Baets, "Electrically pumped InP-based microdisk lasers integrated with a nanophotonic silicon-oninsulator waveguide circuit," Opt. Express 15(11), 6744-6749 (2007).

[12] A. Yariv, "Critical coupling and its control in optical waveguide-ring resonator systems," IEEE Photon. Technol. Lett. 14 (4), 483-485 (2004)

[13] M. Fujita, A. Sakai, and T. Baba, "Ultrasmall and Ultralow Threshold GaInAsP-InP Microdisk Injection Lasers: Design, Fabrication, Lasing Characteristics, and Spontaneous Emission Factor," IEEE J. Select. Topics Quantum Electron. 5(3), 673-681 (1999).

[14] J. Van Campenhout, L. Liu, P. Rojo-Romeo, D. Van Thourhout, C. Seassal, P. Regreny, L. Di Cioccio, J.-M. Fedeli, R. Baets, "A Compact SOI-Integrated Multiwavelength Laser Source Based on Cascaded InP Microdisks," IEEE Photon. Technol. Lett. 20(16), 1345-1347 (2008).

[15] C. Manolatou, M. J. Khan, S. Fan, P. R. Villeneuve, H. A. Haus, and J. D. Joannopoulos, "Coupling of Modes Analysis of Resonant Channel Add-Drop Filters," IEEE J. Quantum Electron. 35(9), 1322-1331 (1999).

[16] J. V. Campenhout, P. Rojo-Romeo, D. V. Thourhout, C. Seassal, P. Regreny, L. D. Cioccio, J. M. Fedeli, and R. Baets, "Thermal characterization of electrically injected thin-film InGaAsP microdisk lasers on Si," J. Lightw. Technol. 25(6), 1543–1548 (2007).

[17] C. H. Henry, "Theory of the Linewidth of Semiconductor Lasers," IEEE J. Quantum Electron. 18(2), 259-264 (1982).

Back to Title List [Search This Volume]

Monday 27 October 2008

PARTIAL TABLE OF CONTENTS

This volume is in progress. Newly published articles are added as they are completed and approved for publication.

Each article is designated by a unique six-digit article number. When citing these articles, the article number should be used instead of a page number; for example, Proc. SPIE 7135, 713502 (2008).

Volume 7135 -- Optoelectronic Materials and Devices III

Yi Luo, Jens Buus, Fumio Koyama, Yu-Hwa Lo, Editors , November 2008

Conference Location: Hangzhou, China **Conference Date:** 27 October 2008

PHOTONIC INTEGRATION I

Technical Abstract Summary Digest

SPIE APOC

Asia-Pacific Optical Communications

26-30 October 2008 • Zhejiang International Conference Center • Hangzhou, China

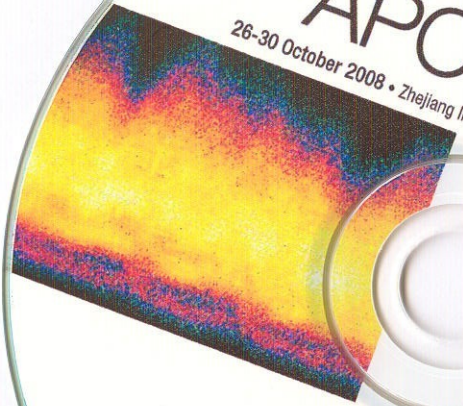

Courtesy of Georgia Intitute of Technology.

SPIE
Chinese Optical Society (COS)
China Institute of Communications (CIC)
Joint Research Center of Photonics of the Royal Institute of Technology (Sweden) and Zhejiang University (China)